Biochimica et Biophysica Acta 1838 (2014) 1701–1709

Contents lists available at ScienceDirect

Biochimica et Biophysica Acta

journal homepage: www.elsevier.com/locate/bbamem

Membrane disorder and phospholipid scrambling in electropermeabilized and viable cells

Jean-Michel Escoffre [a,b,1], Elisabeth Bellard [a,b], Cécile Faurie [c], Sarra C. Sébaï [d], Muriel Golzio [a,b], Justin Teissié [a,b,*], Marie-Pierre Rols [a,b,*]

[a] CNRS, IPBS (Institut de Pharmacologie et de Biologie Structurale), 205 route de Narbonne, F-31077, Toulouse, France
[b] Université de Toulouse, UPS, IPBS, F-31077, Toulouse, France
[c] Matwin-Institut Bergonié, 229 cours de l'Argonne, 33076 Bordeaux cedex, France
[d] Eviagenics, Immeuble Villejuif Biopark, 1 Mail du Professeur Georges Mathé, 94800 Villejuif, France

ARTICLE INFO

Article history:
Received 4 September 2013
Received in revised form 11 February 2014
Accepted 19 February 2014
Available online 26 February 2014

Keywords:
Electropermeabilization
Electroporation
Phospholipid flip-flop
Membrane disorder
Optical imaging

ABSTRACT

Membrane electropermeabilization relies on the transient permeabilization of the plasma membrane of cells submitted to electric pulses. This method is widely used in cell biology and medicine due to its efficiency to transfer molecules while limiting loss of cell viability. However, very little is known about the consequences of membrane electropermeabilization at the molecular and cellular levels. Progress in the knowledge of the involved mechanisms is a biophysical challenge. As a transient loss of membrane cohesion is associated with membrane permeabilization, our main objective was to detect and visualize at the single-cell level the incidence of phospholipid scrambling and changes in membrane order. We performed studies using fluorescence microscopy with C6-NBD-PC and FM1-43 to monitor phospholipid scrambling and membrane order of mammalian cells. Millisecond permeabilizing pulses induced membrane disorganization by increasing the translocation of phosphatidylcholines according to an ATP-independent process. The pulses induced the formation of long-lived permeant structures that were present during membrane resealing, but were not associated with phosphatidylcholine internalization. These pulses resulted in a rapid phospholipid flip/flop within less than 1 s and were exclusively restricted to the regions of the permeabilized membrane. Under such electrical conditions, phosphatidylserine externalization was not detected. Moreover, this electrically-mediated membrane disorganization was not correlated with loss of cell viability. Our results could support the existence of direct interactions between the movement of membrane zwitterionic phospholipids and the electric field.

© 2014 Elsevier B.V. All rights reserved.

1. Introduction

For more than 20 years, the main goal in the development of drug delivery methods has been to increase the effectiveness of existing methods without harming tissue. Among these methods, electropermeabilization has received increasing attention as routine practice for drug delivery in cell biology [1,2] and in medicine [3,4]. This method consists in the controlled application of millisecond long pulsed electric fields (msPEF) on cells in order to transiently increase their native membrane permeability [5]. The main effect of the application of electric fields on cells is the modulation of their transmembrane potential difference ($\Delta\Psi_m$) through the occurrence of a strong field effect across the membrane (i.e., 0.05 V/nm for a 5 nm layer) [6]. This modulation across the cell membrane leads to an asymmetric field distribution [7,8]. Indeed, when the field is applied, $\Delta\Psi_m$ values are higher at the pole facing the positive electrode than at the pole facing the negative one. Under msPEFs [9], permeabilization was detected in the membrane caps facing the two electrodes [10], with membrane permeabilization facing the anode affecting a larger proportion of the membrane than that facing the cathode. These transient and permeant structures are created only in membrane regions facing the electrodes [11,12].

Despite the use of electropermeabilization, there is still a lack of knowledge about structural and dynamic changes induced by the electric field pulse on the plasma membrane [5]. In addition to changes in the electrical conductance and membrane permeability (for review [5]), the main structural membrane alterations of the electropermeabilized mammalian cells are indeed villi and bleb formation [13–15], as well as loss of the membrane asymmetry [16–19]. However, even though the former alterations are reversible and not associated with a loss of cell viability, the latter are permanent and correlated with cell death. The effect of electropermeabilization on

* Corresponding authors at: CNRS, IPBS (Institut de Pharmacologie et de Biologie Structurale), 205 route de Narbonne, F-31077, Toulouse, France.
E-mail addresses: justin.teissie@ipbs.fr (J. Teissié), rols@ipbs.fr (M.-P. Rols).
[1] Present address: Imaging Division, University Medical Center Utrecht, Heidelberglaan 100, P.O. Box 85800, 3508 GA Utrecht, The Netherlands.

http://dx.doi.org/10.1016/j.bbamem.2014.02.013
0005-2736/© 2014 Elsevier B.V. All rights reserved.

membrane asymmetry has only been addressed in erythrocytes [16–19]. Erythrocyte electropermeabilization was described as a two-step process composed of a rapid membrane permeabilization step leading to ion exchange, followed by a dramatic osmotic swelling a few seconds after electropermeabilization. Swelling was accompanied by "crater" formation sustaining hemoglobin leakage that leads to changes in the size and shape of erythrocytes [16,18]. This hemolysis resulted in the formation of ghost cells. Since these ghost cells were both lysed and dead cells, the effect of electropermeabilization on cell viability could not be evaluated. In these studies, electropermeabilization was correlated with an increase in transverse mobility of phospholipids, leading to a perturbation of phospholipid asymmetry [16,19]. Under their experimental conditions, this loss in asymmetry was an irreversible process only correlated with osmotic swelling after electropermeabilization [17,19,20]. Even if erythrocytes are readily used as a simple and convenient way to study biological processes, they have several limits in addressing some basic or applied issues on gene and drug delivery using electropermeabilization. Indeed, erythrocytes have no nucleus, harbor a bi-dimensional actin/spectrin cytoskeleton and are rather different from other mammalian cells. Moreover, no direct observations of what occurred at the plasma membrane level were available and no direct correlations between the phospholipid flip/flop sites and the permeabilized sites could be obtained.

To date, the molecular organization of the membrane during permeabilization still remains unknown [21]. Although some molecular dynamic simulations report the formation of non-polar "pores" in octane and phospholipid bilayers [22,23], a vectorial effect from the transmembrane field on the interfacial dipoles appears to be present [24,25]. The torque (consequence of the electric field on a dipole) creates an opposing directional movement on both sides of the membrane. On one side, the dipole is pulled in an erected configuration, while on the other it is pushed towards the membrane. The transmembrane directions of the electric field are the opposite on the two cell caps [26]. This results in an erected configuration on the outer layer of one cap, and in an embedded configuration on the other cap. In the case of lipid assemblies, the first targets of the field are the charged species present in the proteolipidic membrane. The lipid head group orientation is affected during the electric field application [27]. This appears to be one of the steps triggering the electropulsation process [28]. In the case of mammalian cells, this tilt in the polar head orientation remains present after the pulse as long as the cells are permeabilized [29]. Molecular dynamic simulation of electropermeabilization kinetics showed that this tilt could be induced with high electric fields [21,30]. The relaxation time for this reorientation is in the order of microseconds, but in *in vivo* membranes this would be even slower [31–33]. Indeed, it was found that proteins have a stabilizing effect on phospholipid bilayers in a simulation showing decreased typical "pore" formation times in a protein-free membranes versus a gramicidin–lipid system [34]. This simulation study appeared to show that low external fields affect the dipole orientation much slower than compared to the case when a strong field is applied.

An electric field-induced asymmetry in lipid dipole distribution is present between the two lipid leaflets. However, the kinetics of the dipole orientation will not be the same on both sides of the cell. Indeed, this is observed when cells are exposed to nanosecond pulsed electric fields (nsPEF) almost five times the voltage level generally required for msPEF ($\Delta\Psi_m$ value at the anodic pole cell reaching values of 1.6 V after 15 ns). The $\Delta\Psi_m$ value on the side facing the cathode reached values of 0.6 V in the same time period, indicating a strong asymmetry in conduction mechanisms in the membranes of the two opposite cell hemispheres [35]. Molecular simulations showed that with application of nsPEFs, the phosphatidylcholine (PC) dipoles on the outer layer at the anode side become reoriented, leading to the defect initiation at the outer membrane surface. Under nsPEFs, no PC translocation was described. However, if "pores" are formed, negatively charged phospholipids begin to drift and diffuse towards the exterior surface [36]. Simulations described phosphatidylserine (PS) translocation as a "pore"-facilitated event, rather than as the result of molecular translocation across the transmembrane energy barrier. Indeed, nanosecond PS translocation is the result of an electrophoretic migration of the negatively charged PS head group along the surface of nanometer-diameter "pores" [37]. Under nsPEFs, PS translocation is positively correlated to the membrane permeabilization for the $\Delta\Psi_m$ calculated value of 3.4 V [38]. One open question is the description of the PC dipole as it is indeed a hydrated lipid head group. Water molecules are not only connected to each other by the hydrogen bonds, but they also interact with phospholipids by hydrogen bonds. Interfacial water molecules have been described as highly sensitive to the electric field and able to induce nanometer membrane "pores" under nsPEFs [21,22,30,38,39]. Indeed, Tokman *et al.*, recently reported that under nsPEFs, electropermeabilization is driven by the field-induced reorganization of water dipoles at the water–lipid interface [39]. The interfacial water molecules are the main players (both initiators and drivers) of the electropermeabilization process. The role of the phospholipid bilayer, to a first-order approximation, is then reduced to a relatively passive barrier. However, under our experimental conditions (i.e., millisecond pulse duration, $\Delta\Psi_m$ less than 0.3 V, loading time about 1 μs), the membrane "poration" should take place after the dipole orientation and the tilt of the polar groups, but on a much slower scale. Following the tilt, a collective effect of the water dipoles of the hydrated PC head group may induce its translocation.

The aim of this work was to further investigate the consequences of the application of msPEF on the plasma membrane. Any direct investigation into both spatial and temporal resolutions of the effects of msPEF on phospholipid transverse mobility and membrane order could help in the understanding of the electropermeabilization process. Our strategy consisted of monitoring the transverse mobility of phospholipids in Chinese hamster ovary cells (CHO cells). To detect phospholipid internalization and translocation, the CHO cells were stained with fluorescent probes, C6-NBD-PC (i.e., 1-palmitoyl-2-(7-nitrobenz-2-oxa-1,3-diazol-4-yl-hexanoyl)-sn-glycero-3-PC) and FM1-43 (i.e., N-(3-triethylammoniumpropyl)-4-(4-(dibutylamino)styryl)pyridinium dibromide). This approach provided a direct visualization of transient lipid movement, with spatio-temporal information on the association between the regions of permeabilized membrane and the phospholipid flip/flop sites within them. Fluorescence imaging allowed us to address several questions: (i) Does the application of the electric pulses induce an increase in phospholipid flip/flop in viable nucleated cells? (ii) Is there a direct association between the membrane permeabilization regions and phospholipid flip/flop sites? (iii) Does the electric field play either a direct effector or a simple catalyst role? (iv) Which molecular model(s) can support phospholipid translocation induced by msPEF?

2. Material and methods

2.1. Cell culture

Chinese hamster ovary cells (wild type Toronto clone) were selected for their ability to grow in suspension or on plates. They were grown in MEM medium as previously described [9].

2.2. Electropulsation apparatus

Electropulsation was performed using a CNRS cell electropulsator (PS-10 Jouan, St Herblain, France), which delivered square-wave electric pulses. An oscilloscope (Enertec, St Etienne, France) monitored pulse shape. Stainless steel rod parallel electrodes (diameter 0.5 mm, length 10 mm, inter-electrode distance 7 mm) were connected to the voltage pulse generator [40]. Cells were electropulsed by application of msPEF known to induce macromolecule loading into CHO cells. Ten pulses lasting 5 ms at a frequency of 1 Hz were applied under 0.7 kV/cm at room temperature [41].

2.3. Electropulsation

Cells were cultured on a microscope glass coverslip chamber (Labtek II system, Nunc™, Denmark) at 0.5×10^6 CHO cells per well 1 h before electropulsation to allow them to become attached to the coverslip while still keeping their spherical shape. Cells were electropulsed in 1 mL pulsation buffer (PB) (10 mM K_2HPO_4/KH_2PO_4, 1 mM $MgCl_2$, 250 mM sucrose, pH 7.4) containing propidium iodide (PI) (100 μM) (Sigma-Aldrich®, St-Louis, MO). Propidium iodide uptake was only measured in the regions of the cell chamber where the electric field was homogeneous [10].

2.4. Cell viability

Cell viability was determined by the ability of cells to grow and divide over a 24 h period. Cells were pulsed, kept for 10 min at 37 °C and then grown in Petri dishes in 1 mL of culture medium for 24 h at 37 °C in a 5% CO_2 incubator. Viability was measured by monitoring cell growth using the Crystal Violet assay.

2.5. ATP depletion of CHO cells

Cells were incubated with sodium azide (Sigma-Aldrich®, St-Louis, MO) and 2-deoxy-D-glucose (Sigma-Aldrich®, St-Louis, MO) at 2 mM and 10 mM, respectively, in PBS at 21 °C for 15 min. This optimum condition resulted in a decrease in the ATP content of 75% of its initial value without affecting cell viability as previously described [42].

2.6. C6-NBD-PC membrane probe

C6-NBD-PC (Avanti Polar Lipids, Inc. Alabaster, Alabama) is a diacylglycero-3-phosphatidylcholine molecule where one of the acyl chains is substituted by a fluorescent group, N4-nitrobenzo-2-oxa-1,3-diazole (NBD). Its incorporation into the outer leaflet of the plasma membrane of CHO cells is facilitated by its short acyl chain (only 6 carbon atoms) [43]. Fluorescent vesicles were obtained by mixing 10 μL di-oleoylphosphatidylcholine solution (20 mg/mL) and 20 μL C6-NBD-PC solution (1 mg/mL). A mixed lipid film was obtained by chloroform evaporation in a glass vial under nitrogen flow. The vial was placed in a vacuum for 1 h. The lipid film was resuspended with a 10 mL PBS-Ca^{2+}/Mg^{2+} buffer at 4 °C. The solution was stirred for 1 min followed by sonication for 7 min at 60% of 25 W (VibraCell, Bioblock Scientific, France). 1 h before labeling, cells were cultured on a microscope glass coverslip chamber at 0.5×10^4 CHO cells per well. After three washes with a 1 mL PBS-Ca^{2+}/Mg^{2+} buffer at 4 °C, CHO cells were incubated with 1 mL of fluorescent vesicle solution for 10 min at 4 °C to limit endocytosis. After labeling, CHO cells were washed three times with pulsation buffer to eliminate excess fluorescent vesicles.

2.7. FM1-43 membrane probe

FM1-43 dye (Molecular Probes, Inc., Eugene, Oregon) is a lipophilic styryl compound. The water-soluble FM1-43 dye, which is non-toxic for cells and virtually non-fluorescent in aqueous media, is reported to be inserted into the outer leaflet of the surface membrane where it becomes highly fluorescent [44]. 1 h before labeling cells were cultured on a microscope glass coverslip chamber at 0.5×10^4 CHO cells per well. Cells were washed three times and then mixed with 3 μM FM1-43 in pulsation buffer for 15 min at 37 °C. Cells were directly pulsed in pulsation buffer with FM1-43, without washing as previously described [45].

2.8. Annexin-V

Apoptosis was detected using the Annexin-V assay (Molecular Probes, Inc., Eugene, Oregon). Cells were cultured on a microscope glass coverslip chamber at 0.5×10^4 CHO cells per well 1 h before electropulsation. After electropulsation, the CHO cells were washed three times with an Annexin-V binding buffer and then labeled with 50 μL Annexin-V FITC in the PBS for 15 min at room temperature in the dark. Cells were analyzed using flow cytometry and fluorescence microscopy.

2.9. Fluorescence imaging

For microscopic observations, the microscope glass coverslip chamber carrying the electrodes was placed on the stage of an inverted digitized fluorescence videomicroscope (Leica DMIRB, Wetzlar, Germany). Cells were observed with a Leica 100×, 1.30 oil immersion objective. The wavelengths were selected by using the Leica L4 filter block for the C6-NBD-PC and FM1-43-labeled cells and the Leica N2.1 filter block for PI-labeled cells. Images were recorded with a Photometrics cooled CCD camera (Princeton instrument, Inc., Trenton, NJ, USA) and a computer-controlled excitation light source (Leica, EL 6000, Wetzlar, Germany). The shutter limited photobleaching. Digitized images were processed using MetaMorph Acquisition software (Version 7.04r4 © 1992–2006 Molecular Devices, Downingtown, PA, USA) ran on a DELL computer under Microsoft Windows XP.

2.10. Data analysis

2.10.1. C6-NBD-PC internalization

To quantify C6-NBD-PC internalization for each cell, the mean fluorescence intensities of the membrane and the cytoplasm were determined along a profile line scan as follows. The two maxima of the line scan corresponding to the membrane were detected and their intensity averaged after subtraction of the background. A preview of whole line scans allowed us to choose a threshold of 10 pixels from the maximum indexes in the direction of the cell center as a good compromise to establish the frontier cytoplasm/membrane. This threshold of 10 pixels was, therefore, applied to each analyzed line scan to reach the cytoplasm from the maximum indexes. Thus, after subtraction of the background, measurement of the mean fluorescence in the cytoplasm along the line scan was calculated between these two limits obtained by this threshold. Finally, we calculated the mean fluorescence ratio R between the cytoplasm and the membrane. This ratio was calculated before and after electropulsation, at 0.5 min, 5 min and 10 min. Values after electropulsation were corrected by subtraction of the pre-pulse value.

2.10.2. FM1-43 emission

For quantification of charged phospholipid translocation, surface plots in the pseudo-color of FM1-43 emission were processed by Image J software (a public domain Java image processing program by W. Rasband at NIHM, NIH, Bethesda, MA, USA). Then, mean fluorescence intensities of the plasma membrane facing the anode (I_A) and the cathode (I_C) before ($n = 0$) and during ($n = 10$) electropulsation were determined. Mean intensities were corrected from the background fluorescence. To determine the value of θ_p ($\theta_p = \theta_M / 2$), the fluorescence intensity profile was drawn along the cell membrane. A plot of fluorescence intensity as a function of the polar angle was obtained and its reading gave the value of θ_p. It is the polar reading where no fluorescence change is detected anymore at the equatorial position.

2.11. Statistical analysis

We analyzed at least 100 cells per assay using a delayed image analysis of the stored files. In each figure of this manuscript, we display a representative cell for the cells observed. Errors bars represent the standard error of the mean. The statistical significance of the differences between the means was evaluated by an unpaired Student's *t*-test. All statistics tests were two sided (NS, not significant; $^{*}p < 0.05$; $^{**}p < 0.01$; $^{***}p < 0.001$).

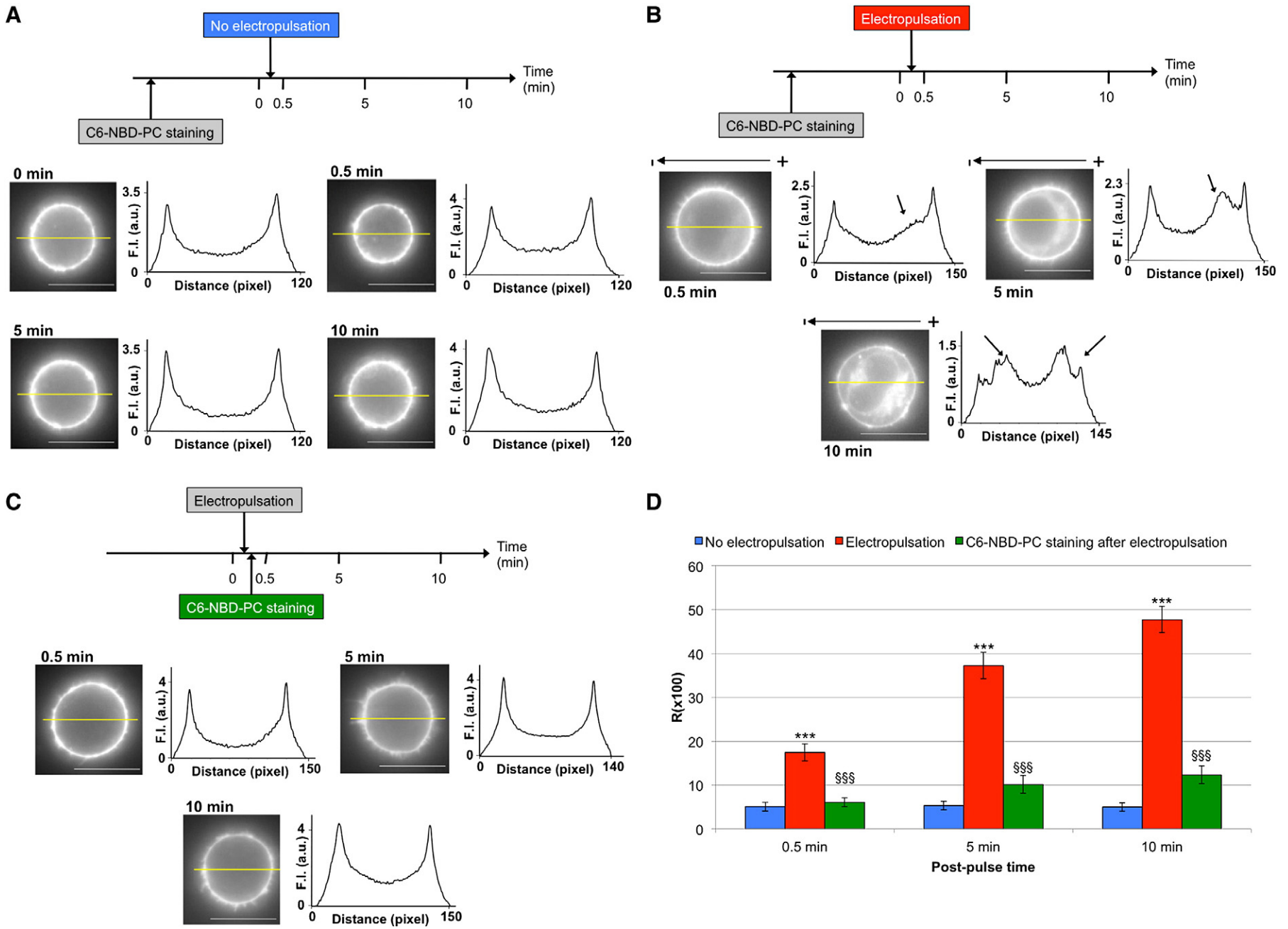
A
No electropulsation
Time (min)
0 0.5 5 10
C6-NBD-PC staining
0 min
0.5 min
5 min
10 min
F.I. (a.u.)
Distance (pixel)
120
B
Electropulsation
Time (min)
0 0.5 5 10
C6-NBD-PC staining
0.5 min
5 min
10 min
F.I. (a.u.)
Distance (pixel)
150
145
C
Electropulsation
Time (min)
0 0.5 5 10
C6-NBD-PC staining
0.5 min
5 min
10 min
F.I. (a.u.)
Distance (pixel)
150
140
D
No electropulsation
Electropulsation
C6-NBD-PC staining after electropulsation
R(x100)
0 10 20 30 40 50 60
***
§§§
0.5 min
5 min
10 min
Post-pulse time

3. Results

We investigated the effects of msPEFs on the transverse mobility of phospholipids by fluorescence digitized videomicroscopy at the single-cell level by using two complementary approaches: (i) To visualize the putative phospholipid internalization within the CHO cells subjected to msPEFs, we labeled the cells with C6-NBD-PC, a PC-like probe. Once inserted into the membrane, C6-NBD-PC does not spontaneously translocate from the outer leaflet to the inner leaflet. However, if transverse movements occur, C6-NBD-PC can freely exchange with intracellular organelle phospholipids. As a consequence, the detection of this probe in the intracellular membrane network, i.e., within the cytoplasm, is indicative of its internalization. (ii) To further investigate phospholipid translocation in CHO cells after the application of msPEFs, FM1-43 was used to detect charged phospholipid translocation and/or membrane assembly changes. The insertion of FM1-43 into the membrane from the bulk is a fast process controlled by a decrease of lipid packing and/or an electrostatic process whereby negatively charged membrane compounds attract the positively charged FM1-43 from the medium into the plasma membrane. The increase in FM1-43 membrane insertion induces a fluorescence overshoot at the affected membrane level. FM1-43 fluorescence gives a local response in the membrane. PS externalization was directly accessed by the Annexin-V test.

3.1. msPEF effects on C6-NDB-PC internalization

In the absence of any electric pulse just after labeling, the C6-NBD-PC was only detected at the plasma membrane level (Fig. 1A and D). The light plot obtained by image analysis confirmed that the maximum intensity was measured at the plasma membrane level (Fig. 1A and D). After 10 min at room temperature, the C6-NBD-PC remained localized at the plasma membrane level (Fig. 1A and D). Bleaching was slightly present under our experimental protocol, but no C6-NBD-PC internalization was observed overtime. The application of a non-permeabilizing electric field pulse (i.e., 0.1 kV/cm, 5 ms) on cells did not affect the probe distribution over time (data not shown).

When cells were subjected to a sequence of 10 electric field pulses (i.e., ""0.7 kV/cm, 5 ms, 1 Hz frequency), all cells were permeabilized as previously observed by our group shown by the uptake of PI. Up to 30 s after application of the first pulse, the C6-NBD-PC localization remained almost unchanged. The radial light plots confirmed the membrane localization of the probe. Nevertheless, a slight and diffuse labeling was seen in the cytoplasm of permeabilized cells (Fig. 1B and D). Overtime, the probe was increasingly present in the organelle membranes, enhancing the detection of the intracellular membrane network (Fig. 1B and D). At 10 min post-pulse, the light plot showed a decrease in the membrane fluorescence level with an increase in the intracellular fluorescence level (Fig. 1B and D). Labeling of the nuclear envelope was observed 10 min after msPEFs application (Fig. 1B Panel C). The total cell fluorescence decreased slightly after electropermeabilization (Fig. 1B). The same results were obtained in ATP-depleted CHO cells (Data not shown). These results are evidence for electropulsation-induced C6-NBD-PC internalization according to an ATP-independent process.

When C6-NBD-PC staining was performed after the application of electric field pulses (i.e., during membrane resealing), no labeling of the intracellular membrane network was observed (Fig. 1C and D). This indicated that the pulse-induced long-lived permeant structures were not associated with PC-like phospholipid internalization.

3.2. Effects of msPEFs on phospholipid scrambling and/or membrane order

Phospholipid scrambling and membrane order were monitored by time-lapse FM1-43 fluorescence microscopy at the single living cell level (Fig. 2). In the absence of any electric pulse, or after non-permeabilizing electric pulses (i.e., 0.1 kV/cm) (data not shown), the FM1-43 fluorescence was only detected in the plasma membrane and intracellular network, as quantified by the surface plot (Fig. 2A, $n = 0$). The application of a permeabilizing electric pulse train induced a fast increase in fluorescence intensity at the membrane regions facing the electrodes (Fig. 2, $n = 1$ to $n = 10$). This fluorescence intensity increased with the number of electric pulses (Fig. 2). Moreover, the fluorescence increase facing the anode was twice that of the one facing the cathode (Fig. 2). This fluorescence intensity local overshoot decayed 1 min after the application of electric pulses (Fig. 2A). The same results were obtained in ATP-depleted CHO cells (Data not shown). Little or no change in the FM1-43 fluorescence inside the cell was observed (Fig. 2). The msPEFs only induced a rapid fluorescence change within less than 1 s (i.e., from the first electric pulses of 5 ms) reflecting thus either electrical changes and/or phospholipid scrambling in the membrane regions facing the electrodes, i.e., where permeabilization took place.

3.3. Effects of msPEFs on cell viability and PS externalization

The msPEFs allowed the transient and reversible permeabilization of CHO cells. Under such experimental conditions, permeabilization took place facing the electrodes and was shown here to be associated with an increase in transbilayer movements of PC phospholipids. This permeabilization was related to a 20% decrease in cell viability at 24 h post-electropermeabilization (Fig. 3). On the other hand, no PS externalization (less than 5% of the Annexin-V positive cells) was detected either in the few minutes or 24 h following membrane electropermeabilization (Fig. 4). Moreover, no morphological alterations such as membrane blebs were observed. If drastic pulsing conditions were applied (10 pulses lasting 5 ms at a frequency of 1 Hz, at 1.2 kV/cm), a total loss in cell viability was observed (i.e., 95% decrease in cell viability at 24 h post-electropermeabilization) (Fig. 4). As a result, PS external exposure was detected in a large proportion of pulsed cells (i.e., $60 \pm 5\%$) within a few minutes post-electropermeabilization. Twenty-four hours after electropermeabilization, more than 80% of pulsed cells showed PS externalization (data not shown). These results showed that the strengths of msPEFs that preserve cell viability additionally do not induce PS externalization.

4. Discussion

In the present study, the effects of msPEFs (i.e., used for gene delivery) on the transverse mobility of phospholipids were directly addressed

Fig. 1. Effect of msPEFs on C6-NBD-PC internalization in CHO cells. A. C6-NBD-PC distribution in CHO cells before electropulsation. The outer leaflet of the plasma membrane was labeled with the C6-NBD-PC probe at 4 °C. The CHO cells were observed at the single-cell level over time. Fluorescent profile graphs represent fluorescence along the cell's diameter (*yellow line*) (F.I., fluorescence intensity). (Scale bar, 15 μm). B. C6-NBD-PC distribution in CHO cells after electropulsation. The outer leaflet of the plasma membrane was labeled with the C6-NBD-PC probe at 4 °C. The CHO cells were observed at the single-cell level following the application of permeabilizing electric pulses (10 pulses lasting 5 ms at a frequency of 1 Hz, at 0.7 kV/cm). Black arrows on graphs show the C6-NBD-PC internalization. Graphs representing the fluorescence profile (*yellow line*) are drawn parallel to electric field lines at the poles facing the electrodes (F.I., fluorescence intensity). (Scale bar, 15 μm). C. C6-NBD-PC staining of CHO cells after electropulsation. The CHO cells were electropermeabilized (10 pulses lasting 5 ms at a frequency of 1 Hz, at 0.7 kV/cm). Afterwards, C6-NBD-PC staining was performed 0.5 min, 5 min and 10 min after electropulsation at 4 °C. Graphs representing the fluorescence profile (*yellow line*) are drawn parallel to electric field lines at the poles facing the electrodes (F.I., fluorescence intensity). (Scale bar, 15 μm). *D*. Quantification of C6-NBD-PC internalization on CHO cells. The mean fluorescence ratio R between the cytoplasm and the membrane was calculated and multiplied by 100. This ratio was calculated before and after electropulsation, at 0.5 min, 5 min and 10 min. Values after electropulsation were corrected by subtraction of a pre-pulse value. Errors bars represent the standard error of the mean. The statistical significance of differences between the means of R for the "no electropulsation" condition and for "electropulsation" condition (NS, not significant; $^{*}p < 0.05$; $^{**}p < 0.01$; $^{***}p < 0.005$) and the means of R for "electropulsation" and for "C6-NBD-PC staining after electropulsation" conditions (NS, not significant; $^{§}p < 0.05$; $^{§§}p < 0.01$; $^{§§§}p < 0.005$) were evaluated by an unpaired Student's *t*-test.

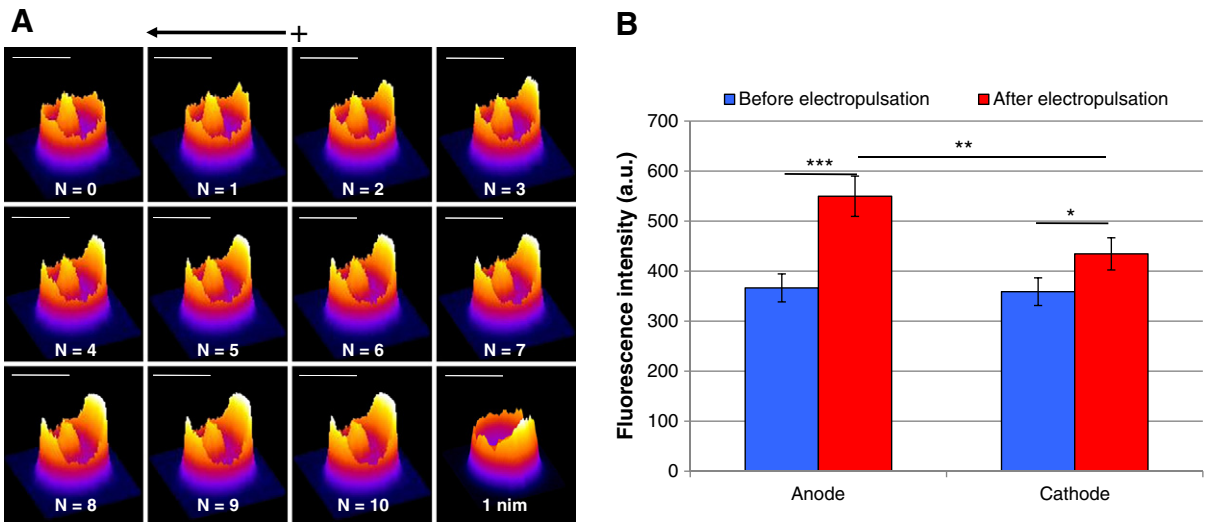

Fig. 2. Effect of msPEFs on phospholipid scrambling in CHO cells. *A.* CHO cells were labeled with FM1-43 at 37 °C. The CHO cells were observed at the single-cell level by fluorescence videomicroscopy during the electropulsation train (10 pulses lasting 5 ms at a frequency of 1 Hz, at 0.7 kV/cm). The surface plot histograms in pseudo-color were obtained by Image J software. (Scale bar, 15 μm). *B.* Quantification of phospholipid scrambling. The mean fluorescence intensities of the membrane facing the electrodes before electropulsation ($n = 0$), during ($n = 1$ to 10) and 1 min after electropulsation train were determined and expressed in percentage (R). Error bars represent the standard error of the mean. The statistical significance of differences between the means of R for the anode and the cathode (NS, not significant; $^{*}p < 0.05$; $^{**}p < 0.01$; $^{***}p < 0.005$) was evaluated by an unpaired Student's *t*-test.

using single CHO cells. Electropermeabilization is a localized process, taking place on the cell caps facing the electrodes [9] under the control of the electric field strength. To determine the biophysical mechanisms involved in this process, we monitored and quantified the pulse-induced transverse mobility of C6-NBD-PC and increased binding of FM1-43 by non-invasive fluorescence digitized time-lapse videomicroscopy.

4.1. Electro-induced phospholipid flip/flop in viable nucleated cells

In gene and drug delivery, cell viability is required to obtain gene expression and to maintain cellular processes. In the present work, all cells were permeabilized under applied msPEF conditions. This permeabilization was transient and related to a 20% decrease in cell viability (Fig. 3). No morphological alterations such as membrane blebs were observed. Under our electrical conditions, PS externalization was not detected either by fluorescence microscopy (Fig. 4A, top panel) or by flow cytometry (Fig. 4B, bottom panel) after Annexin-V staining. This is in contradiction with the results described in previous reports [46]. The limited sensitivity of the Annexin-V assay (a conventional assay) could explain the absence of PS externalization [47]. Indeed, in our experimental conditions at low electric field strength the PS externalization, if any, might be low and the lipid scrambling of PS could also be repaired by aminophospholipid translocase activity [48].

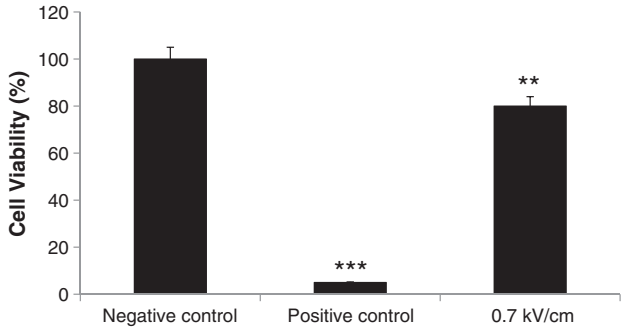

Fig. 3. Cell viability. CHO cells were submitted to 10 pulses lasting 5 ms at a frequency of 1 Hz, at 0.7 kV/cm. Negative and positive controls were respectively performed at 0 kV/cm and 1.2 kV/cm. Cell viability was measured 24 h after electropulsation using Crystal Violet assay. Data expressed as mean ± SEM was calculated from three independent experiments. Statistical analysis was performed using an unpaired Student's *t*-test. Significance was defined as $p < 0.05$ (NS, non-significance, $^{*}p < 0.05$ and $^{***}p < 0.005$ compared to the negative control at 0 kV/cm).

Application of msPEFs induced both PC phospholipid internalization (Fig. 1B) and phospholipid scrambling (Fig. 2). These effects resulted from the permeabilizing nature of electric pulses. These results showed that the application of electropermeabilizing pulses directly altered the phospholipid organization of the plasma membrane by increasing the transverse dynamics of the PC phospholipids according to an ATP-independent process. Enhanced transverse dynamics of PC phospholipids was reported in previous work on erythrocyte ghosts [49]. However, the present observations were obtained using nucleated mammalian cells. These present a significantly different intracellular organization to erythrocytes. In addition, in contrast to erythrocytes where irreversible permeabilization resulted in ghost cell formation (i.e., lysed and dead erythrocytes), cell viability was preserved under our experimental conditions.

4.2. Co-localization between phospholipid scrambling and permeabilized membrane regions

FM1-43 fluorescence changes were present on the two cell caps facing the electrodes. In experiments performed with nanosecond electric pulses, phospholipid scrambling was an asymmetrical process that was restricted to the membrane areas facing the anode [38,46]. In order to determine whether phospholipid scrambling was limited to electropermeabilized regions, we measured the experimental value of the cap angle θp from electropulsation (assayed by PI uptake) and phospholipid scrambling (assayed by FM1-43). These two values were compared. For both processes, the experimental values for angle θp were similar (55° ± 5° and 50° ± 5°, respectively). These data supported the conclusion that phospholipid scrambling was strictly restricted to the permeabilized membrane regions (Fig. 2). This means that the structural events were different from those observed with nsPEFs [38,46].

In light of earlier studies, the asymmetric nature of the observed fluorescence intensity overshoot could confirm that the structure of the permeabilized membrane at the anode pole was different from that found at the cathode pole [50,51], as previously shown in lipid vesicles [12]. These previous studies on small molecule uptake via electropulsation suggested that "electropores" were created on both caps of the cell facing the electrodes, with a smaller "pore" size (but

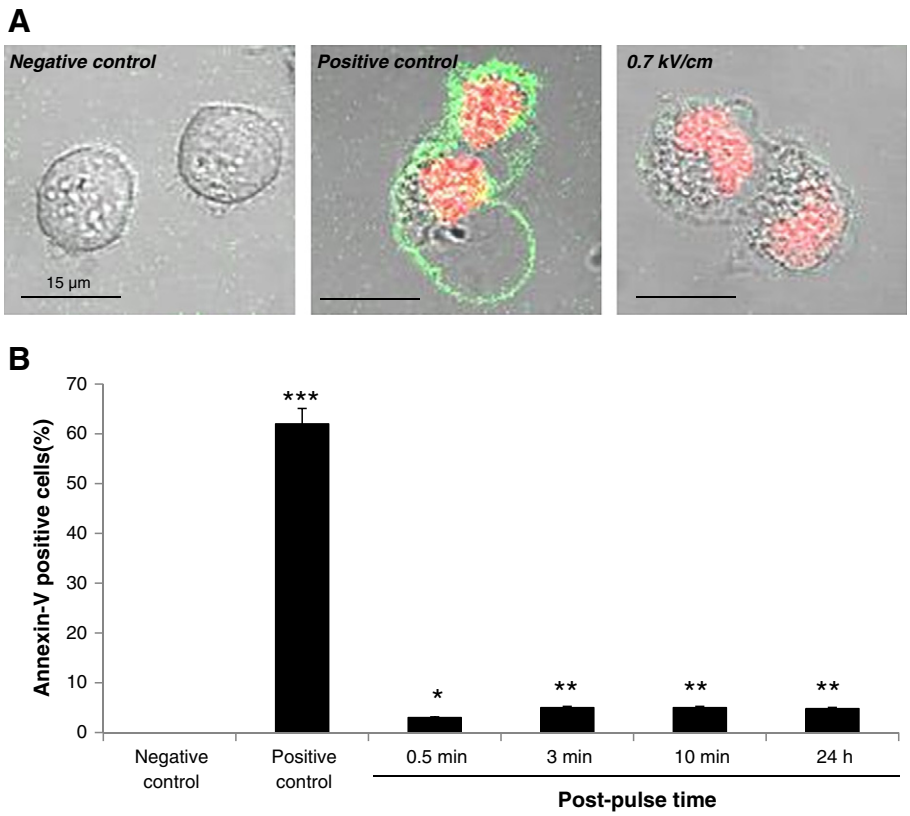

Fig. 4. Lack of msPEFs effect on PS externalization in CHO cells. CHO cells were submitted to 10 pulses lasting 5 ms at a frequency of 1 Hz, at 0.7 kV/cm. *A*. Annexin-V positive cells was observed 0.5 min after electropulsation by confocal microscopy after Annexin-V staining. *B*. The percentage of Annexin-V positive cells was detected 0.5 min, 3 min and 10 min after electropulsation by flow cytometry after Annexin-V staining. Negative and positive controls were respectively performed at 0 kV/cm and 1.2 kV/cm. *B*. Cell viability was measured 24 h after electropulsation using Crystal Violet assay. Data expressed as mean ± SEM was calculated from three independent experiments. Statistical analysis was performed using an unpaired Student's *t*-test. Significance was defined as $p < 0.05$ (NS, non-significance, $^{*}p < 0.05$ and $^{***}p < 0.005$ compared to the negative control at 0 kV/cm).

greater number) on the anode side and larger "pores" (with a lower number) on the cathode side [11]. This asymmetrical process was associated with a vectorial effect of the electric field on the plasma membrane [50]. Depending on their charge, membrane-embedded molecules could either be driven into the cell or pulled out into the outer leaflet of the membrane. Due to the significant structural change in the membrane surface, charges inside and outside the cell could affect the distribution of the transmembrane voltage [26,35]. A simple linear estimation based on the Gaussian law ($\oiint_{\Lambda} D\, d\Lambda$), applied to a 5 nm thick phospholipid bilayer judges that a change of approximately 1000 elementary changes per μm^2 causes a transmembrane potential change of about 100 mV [35].

4.3. Electric field, a direct effector of phospholipid scrambling

The phospholipid scrambling was a direct consequence of electric field pulses and was not due to the enduring leaky membrane organization (Fig. 1B and C). Indeed, in the case of C6-NBD-PC internalization, a progressive staining of the intracellular membrane network was observed after the application of the electric field (Fig. 1B). Nevertheless, when the C6-NBD-PC staining of cells was performed after the application of msPEFs (i.e., during membrane resealing), no labeling of the intracellular membrane network (i.e., probe internalization) was detected (Fig. 1C). Furthermore, the FM1-43 experiments showed that a fluorescence intensity overshoot took place in the permeabilized regions as a direct result of the application of msPEFs (Fig. 2). This fluorescence increase dissipated in the minutes following msPEFs (Fig. 2), which could be explained by lateral diffusion of the perturbation along the cell plasma membrane or by the membrane resealing (returning the controlled membrane organization). These results support the conclusion that a direct interaction was present between the external electric field pulse and the phospholipids under both high electric field and ultrashort pulses [36,46]. Previous reports were observed under more stringent conditions where the organization of interfacial water was strongly affected [52], but were predicted (see the theoretical results) on a slower time scale under our conditions [21].

4.4. Putative molecular mechanisms

From a molecular point of view, our data could be interpreted via two possible mechanisms: Firstly, membrane defects created by electric pulses could provide a new pathway for phospholipids to migrate between the membrane leaflets [19,49] by creating a lipid continuity between the outer and inner leaflets along the toroidal pore, as postulated by the "electroporation theory" [53]. Secondly, electric pulses could cause phospholipid translocation by a direct torque on the head group dipole [36,37].

Model 1 "Electropore"-facilitated phospholipid translocation: In agreement with permeabilization results, "electropores" should be created in permeabilized regions (Fig. 2), but they should remain present during the resealing (as long as "pores" were present). However, no transmembrane movement was observed after the pulse, as shown by the post addition of the C6-NBD-PC, although permeabilization was still present for 10 min. Therefore, this absence of phospholipid flip/flop after the application of msPEFs gave experimental evidence that the pulse-induced long-lived "pores" could not be the pathway for phospholipid exchange between the two membrane leaflets in the permeabilized regions [19,54]. Therefore, only

short-term "electropores" present during pulse application could be the pathway for phospholipid flip/flop. However, the post-pulse "electropores" present during the membrane resealing could not sustain phospholipid translocation, which would be in agreement with previous work [55]. No polar head control of the translocation should be present while PS is not affected. We should however point out that this model of lipid continuity between the two leaflets might be a valid explanation for the processes in erythrocytes, where large "craters" were detected.

Model 2 Phospholipid translocation across the membrane energy barrier: The second model suggests a direct interaction between the external electric field and the phospholipids previously described [21,36]. Phospholipids have been described as the key targets of electric field-mediated permeabilization [56]. In our electrical conditions, the transmembrane field was approximately 0.05 V/nm (for a 5 nm bilayer). This transmembrane field could induce a tilt in the polar head orientation, as previously described in molecular dynamics simulations [21] and experimental data [27,29]. Indeed, in the case for PC, the hydrated head group contains a dipole with a positive charge on the choline and a negative charge carried by the phosphate group. In the absence of an external electric field, lipid dipoles present a random orientation due to the interfacial charges [36,57]. During the induction step of electropulsation (a microsecond process due to the charging time of the membrane, t is about 1 ms), the electric field could induce membrane defects by tilting the lipid dipoles relative to the surface of the membrane [5,58]. Molecular dynamics and coarse-grained simulations only described a large deformation in the bilayer structure to accommodate the transfer of the large PC head groups during flip-flop in a sub-microsecond time scale [59,60]. Water molecules have been described as highly sensitive for the electric field [61] and able to induce membrane defects under the electric field [21,30,38]. Following the tilt of lipid dipoles [21,22,33], a collective effect of water dipoles of hydrated PC head groups might have induced their translocation under our experimental conditions (i.e., msPEFs) (Fig. 1B). Translocation of PC molecules would result in a change in lipid packing on the outer layer (scrambling as shown by the FM1-43). If aqueous defects do form, the translocation of PC would be amplified and the negatively charged lipids (e.g., PS) would begin to drift and diffuse towards the exterior surface [36]. Simulations (on a nanosecond scale or by coarse-grained model) described PS translocation as a nanopore facilitated (i.e., very fast) -event, rather than as the result of molecular translocation across the transmembrane energy barrier [36]. Therefore, the charged phospholipid externalization would only occur in the permeabilized region facing the anode during the application of electric pulses [38,46]. PS externalization has been only reported for high electric fields [37,38,62]. Under our electrical conditions, PS externalization is not detected by the Annexin-V assay, thus suggesting that the electric field intensity is not high enough to induce such a phenomenon.

In addition, the FM1-43 fluorescence overshoot was also detected in the permeabilized region facing the cathode (Fig. 2). This fluorescence overshoot could be interpreted by FM1-43 insertion into a disordered membrane by the electric field (i.e., decrease of lipid packing suggested to be induced by the PC translocation) [56,63]. This result may indicate that msPEFs induced membrane disorder and phospholipid scrambling in the permeabilized regions facing the electrodes, with a larger effect in the permeabilized region facing the anode [64]. This putative mechanism supports a direct interaction between the external electric field and the phospholipids, but in a different way versus microseconds/nanoseconds and high field pulses (i.e., >1 kV/cm). Here, PS translocation takes place only under drastic transmembrane field conditions and the cell viability is dramatically affected. This is in line with previous experiments carried out on Jurkat T cells, where 7 ns pulses caused PS translocation only with field strengths above 2 MV/m, with almost no response to 1 MV/m pulses [45]. In addition, a recent publication reported that calcium and phosphatidylserine inhibit lipid "electropore" formation and reduce pore lifetime [65].

5. Conclusion

In summary, in contrast to non-permeabilizing electrical conditions, permeabilizing msPEFs resulted in membrane disorganization by increasing transverse dynamics of phosphatidylcholines according to an ATP-independent process. Phosphatidylcholine translocation did not occur during the membrane resealing phase. The msPEFs also induced a rapid phospholipid scrambling within less than 1 s that was strictly restricted to the permeabilized regions of the plasma membrane. Moreover, our results did not support PS externalization in our electrical conditions. Thus, these results could suggest the existence of direct interactions between the movement of membrane phospholipids and the electric field. Finally, the enhancement of phospholipid flip-flop and membrane disorder was not correlated to the significant loss of cell viability in the hours following electropermeabilization.

Acknowledgments

The authors thank S. Orlowski, P.F. Devaux and A. Lopez for fruitful discussions, S. Mazères for his help in C6-NBD-PC labeling, and C. Millot for help with cell culture. This work was performed with the "Toulouse Réseau Imagerie" core IPBS facility (Génotoul, Toulouse, France). Dr. J. Butterworth professionally proofread and edited the manuscript (Word Perfect Science, http://www.wordperfectscience.com). The Association Française contre les Myopathies and ANR Astrid PIERGEN (#ANR−12−ASTR−0039−01) (MPR), the Midi-Pyrénées Region, the Direction Générale des Armées and the Institut National du Cancer (JT) have financially supported this work. JM Escoffre was the recipient of an Allocation de Recherche du Ministère de l'Enseignement Supérieur et de la Recherche. This research project was conducted in the scope of EBAM European Associated Laboratory (EAL) and resulted from the networking efforts of the COST Action TD1104 (http://www.electroporation.net).

The authors declare no conflict of interest.

Author's contributions

JME is responsible for the design of experiments, performance of all experiments, analysis of data, and writing of the manuscript. EB assisted in the quantification of data and participated in writing the manuscript. CF, SCS and MG initiated the work. JT is responsible for analysis of data and writing the manuscript. MPR supervised this work and reviewed the manuscript.

References

[1] M. Golzio, M.P. Rols, J. Teissie, In vitro and in vivo electric field-mediated permeabilization, gene transfer, and expression, Methods 33 (2004) 126–135.
[2] M. Cemazar, M. Golzio, J.M. Escoffre, B. Couderc, G. Sersa, J. Teissie, In vivo imaging of tumor growth after electrochemotherapy with cisplatin, Biochem. Biophys. Res. Commun. 348 (2006) 997–1002.
[3] J.M. Escoffre, M.P. Rols, Electrochemotherapy: progress and prospects, Curr. Pharm. Des. 18 (2012) 3406–3415.
[4] A.I. Daud, R.C. DeConti, S. Andrews, P. Urbas, A.I. Riker, V.K. Sondak, P.N. Munster, D.M. Sullivan, K.E. Ugen, J.L. Messina, R. Heller, Phase I trial of interleukin-12 plasmid electroporation in patients with metastatic melanoma, J. Clin. Oncol. 26 (2008) 5896–5903.
[5] J. Teissie, M. Golzio, M.P. Rols, Mechanisms of cell membrane electropermeabilization: a minireview of our present (lack of ?) knowledge, Biochim. Biophys. Acta 1724 (2005) 270–280.

[6] J.M. Escoffre, D.S. Dean, M. Hubert, M.P. Rols, C. Favard, Membrane perturbation by an external electric field: a mechanism to permit molecular uptake, Eur. Biophys. J. 36 (2007) 973–983.
[7] E. Tekle, R.D. Astumian, P.B. Chock, Electro-permeabilization of cell membranes: effect of the resting membrane potential, Biochem. Biophys. Res. Commun. 172 (1990) 282–287.
[8] M. Hibino, H. Itoh, K. Kinosita Jr., Time courses of cell electroporation as revealed by submicrosecond imaging of transmembrane potential, Biophys. J. 64 (1993) 1789–1800.
[9] M. Golzio, J. Teissie, M.P. Rols, Direct visualization at the single-cell level of electrically mediated gene delivery, Proc. Natl. Acad. Sci. U. S. A. 99 (2002) 1292–1297.
[10] B. Gabriel, J. Teissie, Direct observation in the millisecond time range of fluorescent molecule asymmetrical interaction with the electropermeabilized cell membrane, Biophys. J. 73 (1997) 2630–2637.
[11] E. Tekle, R.D. Astumian, P.B. Chock, Selective and asymmetric molecular transport across electroporated cell membranes, Proc. Natl. Acad. Sci. U. S. A. 91 (1994) 11512–11516.
[12] E. Tekle, R.D. Astumian, W.A. Friauf, P.B. Chock, Asymmetric pore distribution and loss of membrane lipid in electroporated DOPC vesicles, Biophys. J. 81 (2001) 960–968.
[13] M.P. Rols, P. Femenia, J. Teissie, Long-lived macropinocytosis takes place in electropermeabilized mammalian cells, Biochem. Biophys. Res. Commun. 208 (1995) 26–35.
[14] M.L. Escande-Geraud, M.P. Rols, M.A. Dupont, N. Gas, J. Teissie, Reversible plasma membrane ultrastructural changes correlated with electropermeabilization in Chinese hamster ovary cells, Biochim. Biophys. Acta 939 (1988) 247–259.
[15] J. Teissie, M.P. Rols, Manipulation of cell cytoskeleton affects the lifetime of cell membrane electropermeabilization, Ann. N. Y. Acad. Sci. 720 (1994) 98–110.
[16] S. Schwarz, B. Deuticke, C.W. Haest, Passive transmembrane redistributions of phospholipids as a determinant of erythrocyte shape change. Studies on electroporated cells, Mol. Membr. Biol. 16 (1999) 247–255.
[17] K. Schwister, B. Deuticke, Formation and properties of aqueous leaks induced in human erythrocytes by electrical breakdown, Biochim. Biophys. Acta 816 (1985) 332–348.
[18] M.M. Henszen, M. Weske, S. Schwarz, C.W. Haest, B. Deuticke, Electric field pulses induce reversible shape transformation of human erythrocytes, Mol. Membr. Biol. 14 (1997) 195–204.
[19] V. Dressler, K. Schwister, C.W. Haest, B. Deuticke, Dielectric breakdown of the erythrocyte membrane enhances transbilayer mobility of phospholipids, Biochim. Biophys. Acta 732 (1983) 304–307.
[20] D.C. Chang, T.S. Reese, Changes in membrane structure induced by electroporation as revealed by rapid-freezing electron microscopy, Biophys. J. 58 (1990) 1–12.
[21] R.A. Bockmann, B.L. de Groot, S. Kakorin, E. Neumann, H. Grubmuller, Kinetics, statistics, and energetics of lipid membrane electroporation studied by molecular dynamics simulations, Biophys. J. 95 (2008) 1837–1850.
[22] D.P. Tieleman, The molecular basis of electroporation, BMC Biochem. 5 (2004) 10.
[23] M.J. Ziegler, P.T. Vernier, Interface water dynamics and porating electric fields for phospholipid bilayers, J. Phys. Chem. B 112 (2008) 13588–13596.
[24] I. Genco, A. Gliozzi, A. Relini, M. Robello, E. Scalas, Electroporation in symmetric and asymmetric membranes, Biochim. Biophys. Acta 1149 (1993) 10–18.
[25] A. Diederich, G. Bähr, M. Winterhalter, Influence of polylysine on the rupture of negatively charged membrane, Langmuir 14 (1998) 4597–4605.
[26] A.G. Pakhomov, A.M. Bowman, B.L. Ibey, F.M. Andre, O.N. Pakhomova, K.H. Schoenbach, Lipid nanopores can form a stable, ion channel-like conduction pathway in cell membrane, Biochem. Biophys. Res. Commun. 385 (2009) 181–186.
[27] G. Stulen, Electric field effects on lipid membrane structure, Biochim. Biophys. Acta 640 (1981) 621–627.
[28] M. Schmeer, T. Seipp, U. Pliquett, S. Kakorin, E. Neumann, Mechanism for the conductivity changes caused by membrane electroporation of CHO cell-pellets, Phys. Chem. Chem. Phys. 6 (2004) 5564–5574.
[29] A. Lopez, M.P. Rols, J. Teissie, ^{31}P NMR analysis of membrane phospholipid organization in viable, reversibly electropermeabilized Chinese hamster ovary cells, Biochemistry 27 (1988) 1222–1228.
[30] P.T. Vernier, M.J. Ziegler, Nanosecond field alignment of head group and water dipoles in electroporating phospholipid bilayers, J. Phys. Chem. B 111 (2007) 12993–12996.
[31] R. Benz, U. Zimmermann, The resealing process of lipid bilayers after reversible electrical breakdown, Biochim. Biophys. Acta 640 (1981) 169–178.
[32] S. Raffy, J. Teissie, Insertion of glycophorin A, a transmembraneous protein, in lipid bilayers can be mediated by electropermeabilization, Eur. J. Biochem. 230 (1995) 722–732.
[33] M. Tarek, Membrane electroporation: a molecular dynamics simulation, Biophys. J. 88 (2005) 4045–4053.
[34] S.W. Siu, R.A. Bockmann, Electric field effects on membranes: gramicidin A as a test ground, J. Struct. Biol. 157 (2007) 545–556.
[35] W. Frey, J.A. White, R.O. Price, P.F. Blackmore, R.P. Joshi, R. Nuccitelli, S.J. Beebe, K.H. Schoenbach, J.F. Kolb, Plasma membrane voltage changes during nanosecond pulsed electric field exposure, Biophys. J. 90 (2006) 3608–3615.
[36] Q. Hu, R.P. Joshi, K.H. Schoenbach, Simulations of nanopore formation and phosphatidylserine externalization in lipid membranes subjected to a high-intensity, ultrashort electric pulse, Phys. Rev. E Stat. Nonlinear Soft Matter Phys. 72 (2005) 031902.
[37] P.T. Vernier, M.J. Ziegler, Y. Sun, M.A. Gundersen, D.P. Tieleman, Nanopore-facilitated, voltage-driven phosphatidylserine translocation in lipid bilayers—in cells and in silico, Phys. Biol. 3 (2006) 233–247.
[38] P.T. Vernier, M.J. Ziegler, Y. Sun, W.V. Chang, M.A. Gundersen, D.P. Tieleman, Nanopore formation and phosphatidylserine externalization in a phospholipid bilayer at high transmembrane potential, J. Am. Chem. Soc. 128 (2006) 6288–6289.
[39] M. Tokman, J.H. Lee, Z.A. Levine, M.C. Ho, M.E. Colvin, P.T. Vernier, Electric field-driven water dipoles: nanoscale architecture of electroporation, PLoS One 8 (2013) e61111.
[40] S. Mazeres, D. Sel, M. Golzio, G. Pucihar, Y. Tamzali, D. Miklavcic, J. Teissie, Non invasive contact electrodes for in vivo localized cutaneous electropulsation and associated drug and nucleic acid delivery, J. Control. Release 134 (2009) 125–131.
[41] C. Rosazza, J.M. Escoffre, A. Zumbusch, M.P. Rols, The actin cytoskeleton has an active role in the electrotransfer of plasmid DNA in mammalian cells, Mol. Ther. 19 (2011) 913–921.
[42] M.P. Rols, C. Delteil, M. Golzio, J. Teissie, Control by ATP and ADP of voltage-induced mammalian-cell-membrane permeabilization, gene transfer and resulting expression, Eur. J. Biochem. 254 (1998) 382–388.
[43] M. Julien, J.F. Tournier, J.F. Tocanne, Differences in the transbilayer and lateral motions of fluorescent analogs of phosphatidylcholine and phosphatidylethanolamine in the apical plasma membrane of bovine aortic endothelial cells, Exp. Cell Res. 208 (1993) 387–397.
[44] M.A. Gaffield, W.J. Betz, Imaging synaptic vesicle exocytosis and endocytosis with FM dyes, Nat. Protoc. 1 (2006) 2916–2921.
[45] P.T. Vernier, Y. Sun, M.A. Gundersen, Nanoelectropulse-driven membrane perturbation and small molecule permeabilization, BMC Cell Biol. 7 (2006) 37.
[46] P.T. Vernier, Y. Sun, L. Marcu, C.M. Craft, M.A. Gundersen, Nanoelectropulse-induced phosphatidylserine translocation, Biophys. J. 86 (2004) 4040–4048.
[47] S.K. Dasgupta, P. Guchhait, P. Thiagarajan, Lactadherin binding and phosphatidylserine expression on cell surface-comparison with annexin A5, Transl. Res. 148 (2006) 19–25.
[48] E. Tekle, M.D. Wolfe, H. Oubrahim, P.B. Chock, Phagocytic clearance of electric field induced 'apoptosis-mimetic' cells, Biochem. Biophys. Res. Commun. 376 (2008) 256–260.
[49] C.W. Haest, D. Kamp, B. Deuticke, Transbilayer reorientation of phospholipid probes in the human erythrocyte membrane. Lessons from studies on electroporated and resealed cells, Biochim. Biophys. Acta 1325 (1997) 17–33.
[50] B. Gabriel, J. Teissie, Mammalian cell electropermeabilization as revealed by millisecond imaging of fluorescence changes with the electropermeabilized cell membrane, Bioelectrochemistry 47 (1998) 113–118.
[51] M.N. Teruel, T. Meyer, Electroporation-induced formation of individual calcium entry sites in the cell body and processes of adherent cells, Biophys. J. 73 (1997) 1785–1796.
[52] U. Pliquett, R.P. Joshi, V. Sridhara, K.H. Schoenbach, High electrical field effects on cell membranes, Bioelectrochemistry 70 (2007) 275–282.
[53] E. Neumann, A.E. Sowers, C.A. Jordan, Electroporation and Electrofusion in Cell Biology, 1989.
[54] A.A. Gurtovenko, I. Vattulainen, Lipid transmembrane asymmetry and intrinsic membrane potential: two sides of the same coin, J. Am. Chem. Soc. 129 (2007) 5358–5359.
[55] G. Pucihar, T. Kotnik, D. Miklavcic, J. Teissie, Kinetics of transmembrane transport of small molecules into electropermeabilized cells, Biophys. J. 95 (2008) 2837–2848.
[56] J. Teissie, T.Y. Tsong, Electric field induced transient pores in phospholipid bilayer vesicles, Biochemistry 20 (1981) 1548–1554.
[57] J. Seelig, P.M. Macdonald, P.G. Scherer, Phospholipid head groups as sensors of electric charge in membranes, Biochemistry 26 (1987) 7535–7541.
[58] M. Kotulska, K. Kubica, S. Koronkiewicz, S. Kalinowski, Modeling the induction of lipid membrane electropermeabilization, Bioelectrochemistry 70 (2007) 64–70.
[59] N. Sapay, W.F. Drew Bennett, D.P. Tieleman, Thermodynamics of flip-flop and desorption for a systematic series of phosphatidylcholine lipids, Soft Matter 5 (2009) 3295–3302.
[60] S.O. Yesylevskyy, L.V. Schafer, D. Sengupta, S.J. Marrink, Polarizable water model for the coarse-grained MARTINI force field, PLoS Comput. Biol. 6 (2010) e1000810.
[61] J. Teissie, Biophysical effects of electric fields on membrane water interfaces: a mini review, Eur. Biophys. J. 36 (2007) 967–972.
[62] R.L. Vincelette, C.C. Roth, M.P. McConnell, J.A. Payne, H.T. Beier, B.L. Ibey, Thresholds for phosphatidylserine externalization in Chinese hamster ovarian cells following exposure to nanosecond pulsed electrical fields (nsPEF), PLoS One 8 (2013) e63122.
[63] U. Schote, J. Seelig, Interaction of the neuronal marker dye FM1-43 with lipid membranes. Thermodynamics and lipid ordering, Biochim. Biophys. Acta 1415 (1998) 135–146.
[64] A. Zweifach, FM1-43 reports plasma membrane phospholipid scrambling in T-lymphocytes, Biochem. J. 349 (2000) 255–260.
[65] Z.A. Levine, P.T. Vernier, Calcium and phosphatidylserine inhibit lipid electropore formation and reduce pore lifetime, J. Membr. Biol. 245 (2012) 599–610.